

Optical properties of fully and partially fluorinated rubrene in films and solution

F. Anger,¹ R. Scholz,² E. Adamski,¹ K. Broch,¹ A. Gerlach,¹ Y. Sakamoto,³ T. Suzuki,³ and F. Schreiber^{1,a)}

¹Institut für Angewandte Physik, Universität Tübingen, 72076 Tübingen, Germany

²Institut für Angewandte Photophysik, Technische Universität Dresden, 01069 Dresden, Germany

³Institute for Molecular Science, Myodaiji, Okazaki 444-8787, Japan

(Received 16 October 2012; accepted 13 December 2012; published online 10 January 2013)

We present the optical properties of fully ($C_{42}F_{28}$, PF-RUB) and half-fluorinated ($C_{42}F_{14}H_{14}$, F_{14} -RUB) rubrene, both in thin films and as monomers in solution and compare them to hydrogenated rubrene ($C_{42}H_{28}$, RUB). All three compounds show similar optical absorption bands and photoluminescence line shapes. The results are interpreted with density functional calculations of the orbital energies and time-dependent density functional theory for the HOMO-LUMO transition. Red shifts induced by the surrounding solvent or organic thin films remain much smaller than for polyacenes, in keeping with previous observations for rubrene and existing models for the solvatochromic shifts. © 2013 American Institute of Physics. [<http://dx.doi.org/10.1063/1.4773520>]

A promising way to tune the electronic and optical properties of organic semiconductors is the complete or partial fluorination of the molecular backbone. It also offers the perspective to reduce the sensitivity to oxygen.^{1–5} In particular, the position of the highest occupied molecular orbital (HOMO) and lowest unoccupied molecular orbital (LUMO) can be fine-tuned, but the resulting energies are not necessarily straightforward to predict. Moreover, fluorinated analogues are an obvious choice for structurally compatible donor-acceptor combinations in organic electronics.^{6–8} Interestingly, not many fluorinated analogues of common hydrogenated organic semiconductors have been studied, partly due to their nontrivial synthesis. Consequently, the understanding of these systems remains limited. Rubrene ($C_{42}H_{28}$, RUB) is one of the best organic semiconductors in terms of charge carrier mobilities in single crystals.^{9,10} In order to improve the electronic and optical properties of molecular materials on the basis of RUB, the investigation of different RUB derivatives became of greater interest during the last years.^{5,11,12} The present letter addresses recently synthesized partially and completely fluorinated rubrene.

The synthesis of perfluorinated ($C_{42}F_{28}$, PF-RUB) and half fluorinated ($C_{42}F_{14}H_{14}$, F_{14} -RUB) rubrene, Fig. 1, is described elsewhere.¹³ Note that F_{14} -RUB differs from RUB and PF-RUB by its lower symmetry and associated strong dipole moment. Both fluorinated materials were purified by temperature gradient sublimation. Hydrogenated rubrene ($C_{42}H_{28}$, RUB) was purchased from Arcos and purified by gradient sublimation.

Thin films of the three materials were grown on silicon wafers covered by a native oxide layer using organic molecular beam deposition techniques^{14,15} at a constant growth rate of roughly 2 Å/min. The films were grown under ultra high vacuum conditions with a thickness of 20 nm on substrates kept at room temperature (RT). Under these conditions, RUB thin films are observed to grow amorphous¹⁶ with a predominance of its twisted isomer.^{17–19}

In order to acquire optical spectra of the pristine films, their absorption spectra were studied *in situ* with a Woollam M-2000 spectroscopic ellipsometer²⁰ directly after growth, before notable de-wetting occurs. Photoluminescence (PL) spectra were acquired using a Horiba Jobin Yvon LabRam HR 800 spectrometer with a CCD-1024 × 256-OPEN-3S9 as detector, within two days after growth on smooth samples in a protective atmosphere, as confirmed by complementary investigations with X-ray reflectivity. Excitation for PL was performed using a frequency doubled Nd:YAG-laser at 532 nm (2.33 eV). Solution spectra in dichloromethane (CH_2Cl_2) were obtained using a JASCO V-570 spectrophotometer and a JASCO FP-6600 spectrofluorophotometer, for absorption and for PL measurements, respectively.

Absorption spectra (ϵ_2 for thin films and α/ω for solution) and PL spectra at room temperature of RUB, F_{14} -RUB, and PF-RUB are shown in Fig. 1. The overall shape is remarkably similar. In order to access the vibronic features, the intensity of the PL spectra was divided by a factor $\omega^3 \cdot n^3(\omega)$.²¹ The energetically lowest peak in the absorption spectra of RUB, F_{14} -RUB, and PF-RUB lies at 2.34 eV (2.34 eV), 2.30 eV (2.30 eV), and 2.33 eV (2.30 eV), respectively, in thin films (in solution). In all three spectra, further peaks follow towards higher energies, each with decreasing intensity with a spacing of approximately 0.17 eV. The highest emission peak is found at 2.20 eV (2.21 eV), 2.14 eV (2.12 eV), and 2.20 eV (2.18 eV) for RUB, F_{14} -RUB, and PF-RUB, respectively, in thin films (in solution). Also in luminescence, we observe further peaks with decreasing intensity towards lower energies, each with a similar spacing as in the absorption spectra. Thin film spectra obtained at 77 K (not shown) do not exhibit additional transition bands, compared to those at RT. Both absorption and PL spectra of RUB match literature spectra well.^{3,22,23}

The most intense peaks in the absorption and PL emission spectra of RUB in Figs. 1(a) and 1(d) are known to stem from the corresponding HOMO-LUMO transition, while the equally spaced further peaks belong to a vibronic progression of the same electronic transition.^{18,22–24} Since for

^{a)}frank.schreiber@uni-tuebingen.de.

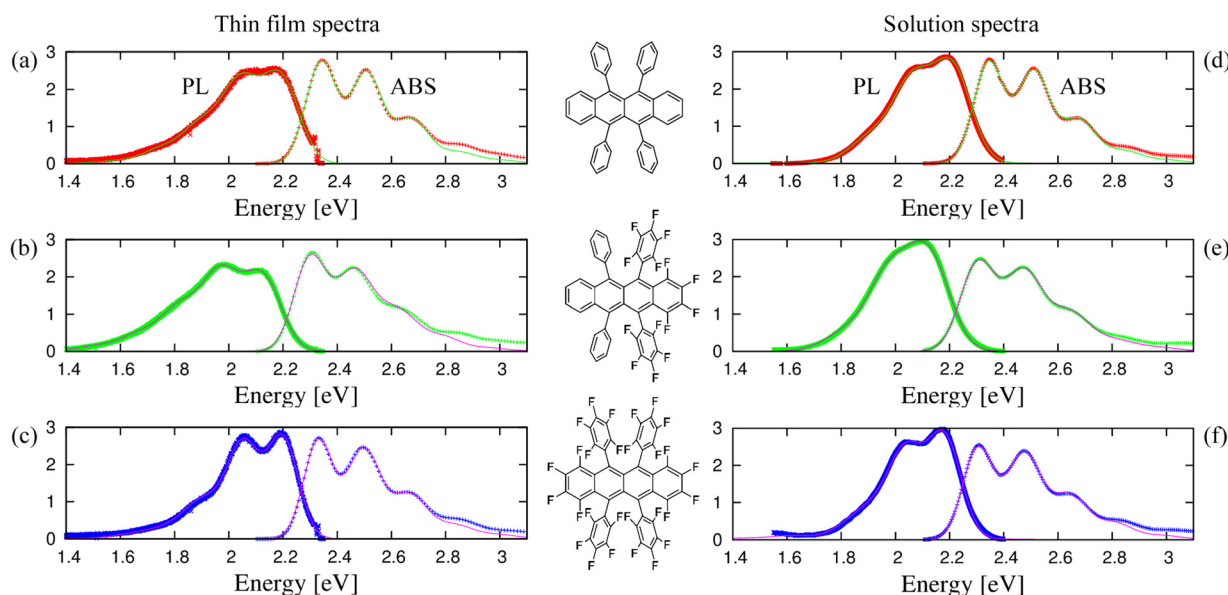


FIG. 1. PL and absorption (ABS, i.e., ϵ_2 in thin films and α/ω in solution) of smooth RUB ($C_{42}H_{28}$), F_{14} -RUB ($C_{42}F_{14}H_{14}$), and PF-RUB ($C_{42}F_{28}$) thin films of 20 nm thickness, (a), (b), and (c), respectively, and in dichloromethane (CH_2Cl_2), (d), (e), and (f), respectively. The PL spectra shown are divided by $\omega^3 n^3(\omega)$ with respect to the measured intensity, giving more direct access to the vibronic progression of an effective internal vibration. The spectra are obtained at RT and for better comparison, their integrated intensity is normalized to 1. Line: Fit according to Eq. (1).

F_{14} -RUB and PF-RUB we do not observe any further peaks within the investigated energy range, also for these materials we assign the most intense peaks in the absorption and PL to the HOMO-LUMO transition and the less intense peaks to the vibronic progression.

As discussed elsewhere in more detail,¹⁸ the shape of the absorption spectrum of RUB is determined by the deformation in the relaxed excited state which can be obtained with density functional theory (DFT). More specifically, a calculated reorganization energy in the excited potential surface of about 0.21 eV can be divided into a contribution of about 0.05 eV arising from low-frequency internal vibrations and about 0.16 eV assigned to internal vibrations of high frequency, clustering around an *effective* mode energy of about 0.17 eV. Therefore, the apparent E_{00} transition of this effective internal mode is expected at about 0.05 eV above the overall E_{00} transition related to the lowest vibrational levels of all internal modes. The spectra in Fig. 1 agree semi-quantitatively with this calculation: For RUB, the difference between the lowest subband of absorption and the highest subband of PL is about $\Delta E_{00} = 0.14$ eV, somewhat larger than 2×0.05 eV = 0.10 eV expected from the contribution of the low-frequency internal modes to the reorganization energies on the ground and excited state potentials. The additional PL redshift of 0.04 eV might arise from thermalization of the excitation towards sites with a particularly low transition energy defined by the local surroundings, modifications of the PL line shape arising from reabsorption,²⁵ or to a principal deficiency of the density functional method chosen previously.¹⁸

The different subbands in absorption and (rescaled) PL depicted in Fig. 1 can be fitted to a Poisson progression over consecutive levels of an effective internal vibration with energy $\hbar\omega_{\text{eff}}$,

$$I(E) = A \sum_n \frac{S^n}{n! \sigma_n \sqrt{2\pi}} \exp \left[-\frac{(E_{00} + n \hbar\omega_{\text{eff}} - E)^2}{2\sigma_n^2} \right], \quad (1)$$

where S is the Huang-Rhys factor of the effective mode. The fit results are shown in Table I, and it turns out that the effective mode has to be chosen slightly differently for absorption and PL. For RUB, the fitted Huang-Rhys factors for absorption and PL are in excellent agreement with the DFT value of $S = 0.985$ for a calculated effective mode at 0.162 eV.¹⁸ This demonstrates that PL from our amorphous films probes the photophysics of monomers, in sharp contrast to the crystalline phase, where intermolecular interactions result in completely different PL spectra.^{22,26} Arithmetically weighting the centers of gravity in absorption ($\langle E_{\text{abs}} \rangle$) and emission ($\langle E_{\text{PL}} \rangle$), we find the experimental HOMO-LUMO transition for RUB, F_{14} -RUB, and PF-RUB thin films at 2.28 eV, 2.21 eV, and 2.28 eV, respectively, for thin films and at 2.30 eV, 2.24 eV, and 2.27 eV for solution. The observed redshift is thereby much lower than the redshift of other organic compounds, e.g., pentacene, which shows a more pronounced redshift from solution to thin film, both in its hydrogenated and in its fluorinated variant.²⁷ However, those molecules form a strict crystalline order, which is not the case for RUB thin films.

Our DFT calculations for the most stable isomers are visualized by a molecular electrostatic potential (MEP) plot mapped on the electron density surface for $0.01/a_B^3$ in Fig. 2. The color coding indicates the inversion of the MEP for RUB and PF-RUB due to the different electron affinity of fluorine and hydrogen. The plot illustrates well the huge dipole moment of F_{14} -RUB, along its backbone. For each of the three compounds under study, two stable isomers can occur, related by an unstable transition state with higher symmetry. In a DFT calculation at the B3LYP/6-31G(d) level as obtained with the Gaussian program package²⁸ for all three cases a geometry with a twisted backbone is the most stable isomer, realizing a D_2 point group for RUB and PF-RUB, and C_2 for F_{14} -RUB, respectively. The DFT results in Table I are reported with respect to the most stable isomer

TABLE I. Fitted values of RUB, F₁₄-RUB, and PF-RUB absorption and emission spectra of the thin films (a) and solution (b). (c) Top: Frontier orbital energy levels of the three model compounds, gap energies, and transition energies obtained with time-dependent DFT for the most stable twisted conformation at the B3LYP/6-31 G(d) level. Bottom: Relative energies of different isomers of the three model compounds. The relative energies are reported with respect to the most stable twisted conformation, including the point group of each isomer.

	RUB	F ₁₄ -RUB	PF-RUB
(a) Thin film			
E_{00}^{abs} (eV)	2.34	2.30	2.33
S_{abs}	0.96	1.00	1.03
$\hbar\omega_{\text{abs}}$ (eV)	0.17	0.16	0.17
$\langle E_{\text{abs}} \rangle$ (eV)	2.50	2.46	2.50
E_{00}^{PL} (eV)	2.20	2.14	2.20
S_{PL}	0.97	1.10	0.95
$\hbar\omega_{\text{PL}}$ (eV)	0.15	0.16	0.15
$\langle E_{\text{PL}} \rangle$ (eV)	2.05	1.96	2.06
(b) Solution			
E_{00}^{abs} (eV)	2.34	2.30	2.30
S_{abs}	0.97	0.97	1.07
$\hbar\omega_{\text{abs}}$ (eV)	0.17	0.17	0.17
$\langle E_{\text{abs}} \rangle$ (eV)	2.50	2.45	2.48
E_{00}^{PL} (eV)	2.21	2.12	2.18
S_{PL}	0.84	0.72	0.91
$\hbar\omega_{\text{PL}}$ (eV)	0.14	0.14	0.14
$\langle E_{\text{PL}} \rangle$ (eV)	2.09	2.03	2.06
(c) DFT calculation			
HOMO (eV)	-4.62	-5.37	-6.09
LUMO (eV)	-2.10	-2.92	-3.67
Gap (eV)	2.52	2.45	2.42
Transition (TD-DFT) (eV)	2.19	2.10	2.06
f_{osc}	0.160	0.146	0.137
Transition dipole [D]	1.73	1.68	1.65
Twisted (eV)	0. (D_2)	0. (C_2)	0. (D_2)
Planar (eV)	0.16 (C_{2h})	0.21 (C_s)	0.30 (C_{2h})
Transition state (eV)	0.28 (D_{2h})	0.29 (C_{2v})	0.51 (D_{2h})

of each molecule. For RUB, the twisted D_2 conformation is 0.16 eV more stable than the C_{2h} isomer resembling the molecular geometry in the crystalline phase, with a D_{2h} isomerization barrier of 0.28 eV between them. With 0.16 eV, the B3LYP energy difference between the two stable isomers is somewhat below the Hartree-Fock/6-31 G(d) value of 0.21 eV found earlier.¹⁹ The isomerization barrier is lower than the Hartree-Fock value of 0.34 eV as well, as expected from previous investigations of torsional potentials involving phenyl groups.²⁹ The perfluorinated compound shows a particularly large stabilization of 0.51 eV with respect to the highly symmetric D_{2h} transition state and of 0.30 eV when compared to the C_{2h} isomer with a planar backbone and tilted fluorinated phenyl groups. In RUB, the stabilization of the D_2 is only 0.28 eV with respect to the D_{2h} transition state, and 0.16 eV with respect to the C_{2h} isomer. The comparison between RUB and PF-RUB reveals that distortions away from the highest symmetry are stabilized by the fluorination, presumably by a steric hindrance between the fluorinated phenyl wings. For RUB and PF-RUB, all isomers have no dipole moment, whereas the dipole moment of F₁₄-RUB

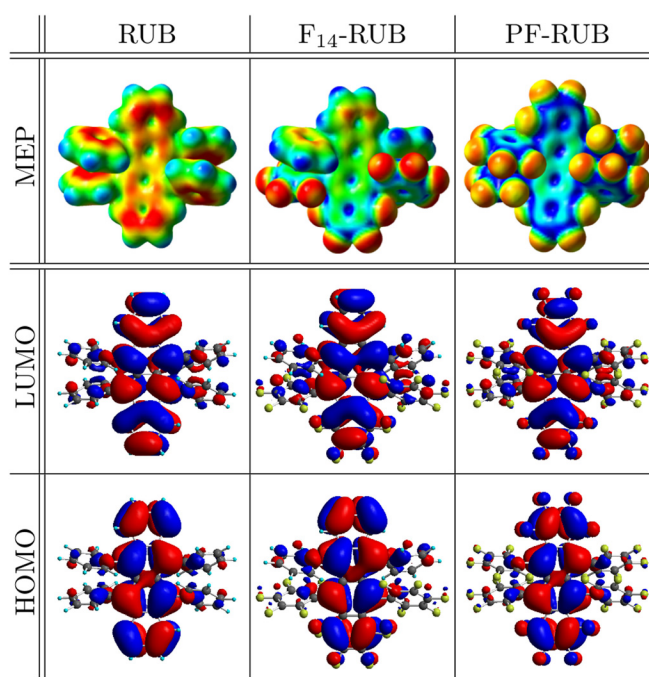


FIG. 2. Molecular electrostatic potential (top) mapped on the electron density surface for $0.01/a_0^3$, with positive potential (blue) close to H atoms and the positively charged core of PF-RUB, and negative potential (red) around F atoms and the negatively charged core of RUB. LUMO (middle) and HOMO (bottom) of RUB, F₁₄-RUB, and PF-RUB in the twisted conformation. Calculated with B3LYP/6-31 G(d).

becomes more pronounced for the less stable isomers: The most stable twisted isomer (C_2) has a dipole moment of 4.22 Debye, growing towards 4.89 Debye (C_s) and 5.10 (C_{2v}). This extraordinarily large dipole moment, which probably is the most fundamental difference to RUB and PF-RUB, suggests that F₁₄-RUB does not just follow a linear interpolation of the (optical) properties of the two other materials.

As expected, the fully or partially fluorinated compounds have significantly lower frontier orbital energies, making the fluorinated variants particularly interesting as acceptor materials for organic solar cells. In F₁₄-RUB, the respective shifts are -0.75 eV (HOMO) and -0.82 eV (LUMO), values roughly doubled for the perfluorinated compound, with -1.47 eV (HOMO) and -1.57 eV (LUMO). From the visualization of the orbitals in Fig. 2, it is obvious that the π and π^* states do not extend significantly over the hydrogen atoms, whereas each fluorine gives a small anti-bonding contribution with a sign change of the orbital along the respective C-F bond.

For F₁₄-RUB and PF-RUB, the absorption and PL spectra resemble hydrogenated RUB. The absorption of F₁₄-RUB shows a significant redshift of about 0.04 eV with respect to RUB, and together with a Stokes shift being larger by 0.04 eV, the PL spectra occur at about 0.08 eV below RUB. Surprisingly, PF-RUB does not shift further to the red, but instead the positions and shapes of absorption and PL spectra are very similar to RUB. Since the “nonlinear” shift (HOMO-LUMO transition energies versus the degree of fluorination of the molecules) occurs also in solution, it is not only a thin film effect.

The general underestimation of the HOMO-LUMO transition of RUB, F₁₄-RUB, and PF-RUB by TD-DFT calculation is a well-known phenomenon for the acene group³⁰ that

resembles the backbone of RUB and its here presented derivatives. However, the monotonous decrease of the frontier orbital energies with increasing fluorination predicted by our DFT calculations reproduces chemical trends observed for other polyaromatic compounds, e.g., partially or fully fluorinated phthalocyanines and polyacenes.^{31,32}

In the emission spectra, reorientation of the dipoles of the solvent can cause an additional redshift of the spectra. For this reason, the further discussion will be restricted to absorption spectra. The redshift $\Delta\nu$ of the absorption spectra of RUB in thin films and solution in comparison to the free molecule due to polarizability differences of ground and excited state molecules can be estimated by an equation following Renge,³³

$$\Delta\nu = p\varphi(n^2), \quad (2)$$

with $\varphi(n^2) = (n^2 - 1)/(n^2 + 2)$, the refraction index n of the solvent, and the slope p of the solvatochromic plot.³³ This results in a solvent shift of -0.06 eV for RUB in CH_2Cl_2 solution ($n^2 \approx 2$) and -0.11 eV for RUB thin films with a refraction index of $n_{\text{RUB}}^2 \approx \epsilon_{1,\text{RUB}} \approx 3.25$ at E_{00} , as obtained from ellipsometry. The latter value is based on the assumption of the RUB thin film as a “solution of RUB molecules in RUB,” which should be a good approximation for disordered thin films, as in the present case. From these values of the solvent shifts and the observed E_{00} transitions in Table I, RUB in CH_2Cl_2 (in the film) yields an estimate of $E_{00} = 2.40$ eV (2.45 eV) in the gas phase. As the solvation cavity of RUB in the thin film might be larger, the solvation shift of -0.11 eV is likely to be somewhat overestimated, so that a gas phase value of $E_{00} = 2.40$ eV seems to be more realistic.

For the other compounds, an evaluation of the solvent shift has to account for the smaller transition dipoles in Table I and an increase of the molecular volume by a factor of 1.17 for F_{14} -RUB and by 1.29 for PF-RUB. As suggested by Bayliss,³⁴ the solvent shift should scale with the squared transition dipole divided by the molecular volume, so that the solvent shift in F_{14} -RUB should be smaller by a factor of about 0.8 and in PF-RUB by a factor of about 0.7. Hence, from the observed E_{00} in solution, both F_{14} -RUB and PF-RUB should have gas phase values close to $E_{00} = 2.35$ eV, and the average vertical transition energies in the gas phase should be about $\langle E_{\text{abs,RUB}} \rangle = 2.56$ eV, $\langle E_{\text{abs,F14-RUB}} \rangle = 2.53$ eV, and $\langle E_{\text{abs,PF-RUB}} \rangle = 2.54$ eV. This estimate for the molecular transition energy of RUB is remarkably close to the calculated B3LYP/6-31 G(d) gap of 2.52 eV, whereas the TD-DFT value for the lowest transition is severely underestimated, a deficiency known from other acenes.³⁰ The calculated DFT gap energy and the lowest transition energy in TD-DFT show stronger chemical trends than the observed spectra, a shortcoming which might be influenced by the poorer convergence of the variational basis for the fluorine-containing compounds. Altogether, taking into account the very large shifts of frontier orbital energies, it is quite remarkable that the optical spectra of the three compounds are so similar. This finding resembles the observed behavior of fluorinated phthalocyanines, but is in sharp contrast to the stronger spectroscopic shifts between pentacene and perfluoropentacene, both in solution and in the crystalline phase.⁸

Overall, the agreement between DFT and experiment is remarkably good, after the shift and corrections by the dielectric environment are considered. This can presumably also be attributed to the amorphous structure of the system that avoids strong crystal effects as observed in the case of fluorinated phthalocyanines or pentacene. Also, the relative similarity of the RUB and PF-RUB spectra is remarkable. Some of the deviations found for F_{14} -RUB within this series may be related to its strong dipole moment, which is yet to be explored and exploited.

To conclude, the optical properties of F_{14} -RUB and PF-RUB have been determined both from thin films and in solution. While the position of the HOMO-LUMO transition of PF-RUB surprisingly resembles the HOMO-LUMO transition of hydrogenated RUB, F_{14} -RUB is slightly redshifted. Due to its strong dipole moment of 4.22 Debye in its most stable conformation, F_{14} -RUB provides a significant potential for applications.

We wish to thank the DFG for the financial support. F. Anger was supported by a Ph.D. fellowship from the Universität Tübingen and K. Broch by the Studienstiftung des Deutschen Volkes.

¹M. Kytka, A. Gerlach, F. Schreiber, and J. Kováč, *Appl. Phys. Lett.* **90**, 131911 (2007).

²X. Song, L. Wang, Q. Fan, Y. Wu, H. Wang, C. Liu, N. Liu, J. Zhu, D. Qi, X. Gao, and A. T. S. Wee, *Appl. Phys. Lett.* **97**, 032106 (2010).

³Y. Harada, T. Takahashi, S. Fujisawa, and T. Kajiwara, *Chem. Phys. Lett.* **62**, 283 (1979).

⁴E. Fumagalli, L. Raimondo, L. Silvestri, M. Moret, A. Sassella, and M. Campione, *Chem. Mater.* **23**, 3246 (2011).

⁵S. Uttiya, L. Raimondo, M. Campione, L. Miozzo, A. Yassar, M. Moret, E. Fumagalli, A. Borghesi, and A. Sassella, *Synth. Met.* **161**, 2603 (2012).

⁶A. Hinderhofer, C. Frank, T. Hosokai, A. Gerlach, A. Resta, and F. Schreiber, *J. Chem. Phys.* **134**, 104702 (2011).

⁷K. Broch, U. Heinemeyer, A. Hinderhofer, F. Anger, R. Scholz, A. Gerlach, and F. Schreiber, *Phys. Rev. B* **83**, 245307 (2011).

⁸F. Anger, J. O. Ossó, U. Heinemeyer, K. Broch, R. Scholz, A. Gerlach, and F. Schreiber, *J. Chem. Phys.* **136**, 054701 (2012).

⁹V. Podzorov, E. Menard, A. Borissov, V. Kiryukhin, J. A. Rogers, and M. E. Gershenson, *Phys. Rev. Lett.* **93**, 086602 (2004).

¹⁰V. C. Sundar, J. Zaumseil, V. Podzorov, E. Menard, R. L. Willett, T. Someya, M. E. Gershenson, and J. A. Rogers, *Science* **303**, 1644 (2004).

¹¹X. T. Zhang, Q. Meng, Y. D. He, C. L. Wang, H. L. Dong, and W. P. Hu, *Sci. China Chem.* **54**, 631 (2011).

¹²H. Fong, S. So, W. Sham, C. Lo, Y. Wu, and C. Chen, *Chem. Phys.* **298**, 119 (2004).

¹³Y. Sakamoto and T. Suzuki (unpublished).

¹⁴G. Witte and C. Wöll, *J. Mater. Res.* **19**, 1889 (2004).

¹⁵F. Schreiber, *J. Phys.: Condens. Matter* **16**, R881 (2004).

¹⁶S.-W. Park, J.-M. Choi, K. H. Lee, H. W. Yeom, S. Im, and Y. K. Lee, *J. Phys. Chem. B* **114**, 5661 (2010).

¹⁷S. Kowarik, A. Gerlach, S. Sellner, F. Schreiber, J. Pflaum, L. Cavalcanti, and O. Konovalov, *Phys. Chem. Chem. Phys.* **8**, 1834 (2006).

¹⁸M. Kytka, L. Gisslen, A. Gerlach, U. Heinemeyer, J. Kováč, R. Scholz, and F. Schreiber, *J. Chem. Phys.* **130**, 214507 (2009).

¹⁹D. Käfer, L. Ruppel, G. Witte, and C. Wöll, *Phys. Rev. Lett.* **95**, 166602 (2005).

²⁰U. Heinemeyer, R. Scholz, L. Gisslén, M. I. Alonso, J. O. Ossó, M. Garriga, A. Hinderhofer, M. Kytka, S. Kowarik, A. Gerlach, and F. Schreiber, *Phys. Rev. B* **78**, 085210 (2008).

²¹R. Loudon, *The Quantum Theory of Light*, 3rd ed. (Oxford University Press, New York, 2000).

²²H. Najafov, I. Biaggio, V. Podzorov, M. F. Calhoun, and M. E. Gershenson, *Phys. Rev. Lett.* **96**, 056604 (2006).

²³O. Mitrofanov, D. V. Lang, C. Kloc, J. M. Wikberg, T. Siegrist, W.-Y. So, M. A. Sergent, and A. P. Ramirez, *Phys. Rev. Lett.* **97**, 166601 (2006).

- ²⁴S.-W. Park, J. M. Hwang, J.-M. Choi, D. K. Hwang, M. S. Oh, J. H. Kim, and S. Im, *Appl. Phys. Lett.* **90**, 153512 (2007).
- ²⁵P. Irkhin, A. Ryasnyanskiy, M. Koehler, and I. Biaggio, *Phys. Rev. B* **86**, 085143 (2012).
- ²⁶M. Müller, A. Langner, O. Krylova, E. L. Moal, and M. Sokolowski, *Appl. Phys. B* **105**, 67 (2011).
- ²⁷A. Hinderhofer, U. Heinemeyer, A. Gerlach, S. Kowarik, R. M. J. Jacobs, Y. Sakamoto, T. Suzuki, and F. Schreiber, *J. Chem. Phys.* **127**, 194705 (2007).
- ²⁸M. J. Frisch, G. W. Trucks, H. B. Schlegel, G. E. Scuseria, M. A. Robb, J. R. Cheeseman, J. A. Montgomery, Jr., T. Vreven, K. N. Kudin *et al.*, Gaussian 03, Revision D.01 (Gaussian, Inc., Wallingford, CT, 2004).
- ²⁹A. Karpfen, C. H. Choi, and M. Kertesz, *J. Phys. Chem. A* **101**, 7426 (1997).
- ³⁰S. Grimme and M. Parac, *ChemPhysChem* **4**, 292 (2003).
- ³¹U. Weiler, T. Mayer, W. Jaegermann, C. Kelting, D. Schlettwein, S. Makarov, and D. Wöhrle, *J. Phys. Chem. B* **108**, 19398 (2004).
- ³²T. Mayer, U. Weiler, C. Kelting, D. Schlettwein, S. Makarov, D. Wöhrle, O. Abdallah, M. Kunst, and W. Jaegermann, *Sol. Energy Mater. Sol. Cells* **91**, 1873 (2007).
- ³³I. Renge, *Chem. Phys.* **167**, 173 (1992).
- ³⁴N. S. Bayliss, *J. Chem. Phys.* **18**, 292 (1950).